Assessment of Regional Cytochrome P450 Activities in Rat Liver Slices Using Resorufin Substrates and Fluorescence Confocal Laser Cytometry

John T. Heinonen, Jaspreet S. Sidhu, Maureen T. Reilly, Federico M. Farin, Curtis J. Omiecinski, David L. Eaton, and Terrance J. Kavanagh

Department of Environmental Health, University of Washington, Seattle, WA 98195 USA

Characterizing constitutive activities and inducibility of various cytochrome P450 isozymes is important for elucidating species and individual differences in susceptibility to many toxicants. Although expression of certain P450s has been studied in homogenized tissues, the ability to assess functional enzyme activity without tissue disruption would further our understanding of interactive factors that modulate P450 activities. We used precision-cut, viable rat liver slices and confocal laser cytometry to determine the regional enzyme activities of P450 isozymes *in situ*. Livers from control and β-naphthoflavone (βNF)-treated rats were sectioned with a Krumdieck tissue slicer into 250-μm thick sections. A slice perfusion chamber that mounts on the cytometer stage was developed to allow for successive measurement of region-specific P450-dependent *O*-dealkylation of 7-ethoxy-, 7-pentoxy-, and 7-benzyloxyresorufin (EROD, PROD, and BROD activity, respectively) in the same liver slice. Images of the accumulated fluorescent resorufin product within the tissue were acquired using a confocal laser cytometer in confocal mode. As expected, slices isolated from βNF-treated rats showed high levels of centrilobular EROD activity compared to slices from control rats, whereas PROD and BROD activities remained at control levels. These techniques should allow for the accurate quantification of regional and cell-specific P450 enzyme activity and, with subsequent analysis of the same slice, the ability to correlate specific P450 mRNAs or other factors with enzymatic activity. Moreover, these techniques should be amenable to examination of similar phenomena in other tissues such as lung and kidney, where marked heterogeneity in cellular P450 expression patterns is also known to occur.
Key words: cytochrome P450, hepatic zones, laser cytometry, liver slices, regional activity. *Environ Health Perspect* 104:536–543 (1996)

Cytochrome P450 monooxygenases (P450s) are a supergene family of enzymes involved in the biotransformation of a wide range of both endogenous and exogenous compounds. P450s play important roles in the metabolism of many drugs and in the activation of a variety of chemical toxicants and carcinogens in both humans and animals (*1,2*). High levels of P450s exist principally in the liver (*1*), and studies using immunohistochemical techniques (*3–6*) and *in situ* hybridization (*7*) have demonstrated differences in the regional distribution and region-specific induction of several P450s within the liver.

Constitutive activities and inducibility of different P450 isozymes are important in dictating species and individual differences in susceptibility to toxicants. The ability to assess gene expression and resulting enzyme activity without tissue disruption on an individual cell basis would further our ability to identify linkages between P450 expression and the zonal distribution of hepatic lesions caused by different toxicants.

Recently, we reported on the use of alkoxyresorufin homologues in combination with noninvasive scanning laser cytometry as a method for directly determining CYP1A1 functional activity in hepatoma cell lines (*8*). In the present study, we used precision-cut, viable rat liver slices and confocal laser cytometry to determine the regional activities of P450 isozymes *in situ*.

A slice perfusion chamber that mounts on the cytometer stage was developed to allow for successive measurement of region-specific, P450-dependent *O*-dealkylation of 7-ethoxy-, 7-pentoxy-, and 7-benzyloxyresorufin (EROD, PROD, and BROD activity, respectively) in the same liver slice. EROD activity in rat liver has been shown to be specific to CYP1A isozymes and is inducible by β-naphthoflavone (βNF) and other polycyclic aromatic hydrocarbon-type inducing agents (*8,9*). BROD and PROD activities have been shown to be specific to CYP2B and CYP3A isozymes and are inducible by phenobarbital (*9,10*). The perfusion system ensures a constant concentration of substrate and limits the extracellular accumulation of the fluorescent product, resorufin (*9*). In addition, the slice perfusion chamber allows for residual substrate and product to be washed away between successive perfusion assays.

Materials and Methods

Chemicals. Earle's balanced salt solution (EBSS) and Williams' E medium were purchased from Gibco BRL (Grand Island, New York). βNF, factor II- and factor VII-deficient rat plasma, rat thrombin, and dicumarol were purchased from Sigma (St. Louis, Missouri). 7-Ethoxy-, 7-pentoxy-, and 7-benzyoloxyresorufin (ER, PR, and BR, respectively) were purchased from Boehringer Mannheim Corp. (Indianapolis, Indiana), and resorufin was purchased from Aldrich Chemical Co. (Milwaukee, Wisconsin).

Animals and slice preparation. Adult, male Sprague-Dawley rats (150–200 g) were purchased from Simenson Labs (Gilroy, California) and were fed Wayne Lablox and given water *ad libitum*. βNF-treated rats were administered 65 mg/kg body weight βNF in corn oil by intraperitoneal injection for 2 consecutive days before sacrifice. Control rats were untreated. The perfusion technique and methods for measurement of alkoxyresorufin *O*-dealkylase activities by scanning confocal laser cytometry were developed during a number of preliminary experiments. Immunocytochemical, microsomal, and dynamic organ culture (DOC) data were obtained from the caudate lobes of a control and a βNF-treated rat. Fluorescence images and slice perfusion data were obtained from the caudate lobes of separate control and βNF-treated rats.

Precision-cut, viable liver slices used in laser cytometry experiments and in DOC experiments were prepared as described by Krumdieck et al. (*11*) using the Krumdieck tissue slicer (K & F Research Co., Birmingham, Alabama). Briefly, animals were killed by ether anesthetization/cervical dislocation. Livers were excised and immediately placed in Williams' E medium containing 10 mM HEPES (pH 7.4; referred to as WEM from this point). An 8-mm metal

Address correspondence to T. J. Kavanagh, Department of Environmental Health, Box 354695, University of Washington, Seattle, WA 98195 USA.
We thank Chen-Ye He for preparing the liver sections used in immunocytochemical staining and Mark Cooper of the Department of Zoology at the University of Washington for helpful discussions on the design of the perfusion chamber. This study was supported by the National Institutes of Health (grants ES-04696, ES-05780, ES-04616, and ES-03933).
Received 24 March 1995; accepted 18 January 1996.

biopsy corer was used to prepare tissue cores from the liver lobes. Cores were then placed in the Krumdieck slicer while submerged in WEM. Optimal slice thickness was previously shown to be 250 µm (*11*). The first and last slices containing the liver capsule were discarded. Liver slices were then placed in DOC vials (2 slices/vial) containing 2 ml of WEM as described by Smith et al. (*12*). Slices were allowed to preincubate for at least 2 hr before use in subsequent perfusion assays or DOC EROD assays.

Slice perfusion. The slice perfusion apparatus shown in Figure 1 was used to successively measure region-specific EROD, PROD, and BROD activities in precision-cut liver slices. A plasma clot similar to that described by Gahwiler (*13*) was formed by evenly distributing 25 µl of reconstituted rat plasma (50 mg/ml PBS, pH 7.4) on a 22-mm square glass cover slip. We then added 10 µl of reconstituted thrombin (117 U/ml in 0.15 M NaCl and 0.05 M sodium citrate, pH 6.5) to the center of the plasma-coated cover slip. The liver slice was then placed on the rapidly formed plasma clot. A cover glass perfusion chamber similar to that described by Forscher et al. (*14*) was formed by suspending the cover slip holding the liver slice over a microscope slide on two 720-µm thick plastic spacers. The spacers and cover slip were held in place by coating spacers with a thin film of silicone grease.

The microscope slide portion of the perfusion chamber was fixed to the cytometer stage by a custom-designed stage mount. The mount positioned the slide over the microscope objective and held reagent supply and vacuum lines in position. Reagent was supplied via 0.58-mm ID polyethylene tubing attached to a 25-ml reservoir positioned approximately 30 cm above the perfusion chamber. A triangular piece of filter paper attached to the vacuum line was positioned on the outlet side of the chamber, as shown in Figure 1, to wick away reagent and provide for a laminar flow of reagent through the chamber. Vacuum and reservoir height were adjusted to establish a flow rate of 0.5 ml/min. Slice perfusion experiments were carried out at room temperature.

EBSS (phenol-red-free, supplemented with 10 mM HEPES, 5 mM $MgCl_2$, and 2.5 mM $CaCl_2$, pH 7.5), gassed with 95% O_2/5% CO_2 and containing 25 µM dicumarol, was used as the perfusion buffer. Dicumarol is a specific inhibitor of quinone oxidoreductase (DT-diaphorase) (*15*), a cytosolic enzyme involved in the reduction of resorufin to a nonfluorescent product. Dicumarol is therefore required in reaction buffers to measure maximum

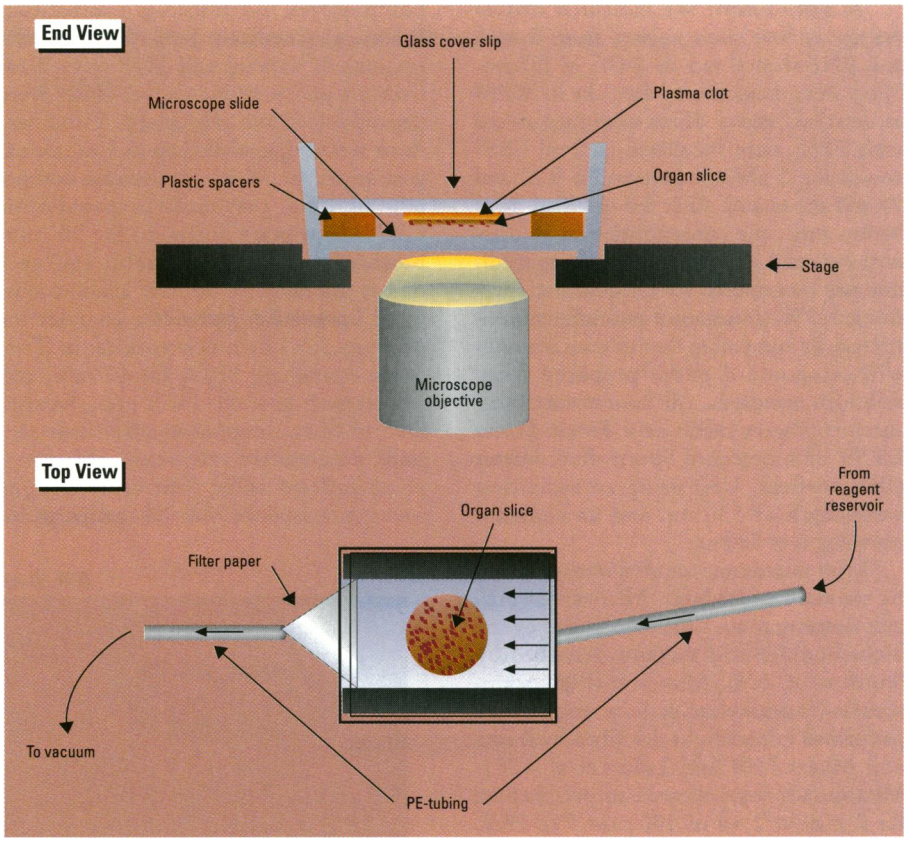

Figure 1. Liver slice perfusion chamber.

alkoxyresorufin *O*-dealkylase activities in hepatic subcellular fractions and hepatocyte homogenates (*16*). We used 25 µM dicumarol in our assays with liver slices, as this concentration was previously found to be optimal for measuring CYP1A1 functional activity in hepatoma cell lines by scanning laser cytometry (*8*). Sulfate anion was omitted from the reaction buffer to minimize conjugation via sulfation (*17*), as previously described (*8*).

We determined region-specific EROD, BROD, and PROD activities by adding the appropriate alkoxyresorufin substrate to the perfusion buffer to a final concentration of 5 µM. EBSS without substrate was used to remove residual substrate and product between successive perfusions. Slices were washed with EBSS until fluorescence returned to baseline levels and was monitored by continuously scanning the liver slice.

Laser cytometry. Alkoxyresorufin *O*-dealkylase activity was assessed directly in liver slices using an ACAS (adherent cell analysis and sorting) Ultima Laser Cytometer (Meridian Instruments, Okemos, Michigan) equipped with an argon ion laser and image analysis software. Initial focusing was carried out by examining the slice with normal transmitted light using a 10× objective. The same objective was used for laser illumination of the slice in confocal mode (pinhole setting of 100 µm). Maximum fluorescence response occurred within the first two to three cell layers from the surface of the slice and could be optimized by scanning in the *Z*-direction upon addition of substrate. Fluorescence due to resorufin formation was monitored using an excitation wavelength of 514 nm and an emission wavelength of >570 nm (using a long-pass dichroic filter). The photomultiplier tube voltage was held constant and data were collected using the kinetics software package supplied with the instrument. Data were analyzed on a DASY 9000 workstation (Meridian Instruments). EROD, BROD, and PROD activities were measured as increases in fluorescence intensity (arbitrary scale) within user-defined polygon regions of the liver slice exhibiting maximum EROD activity. Representative fluorescence pseudocolor images were saved as tagged image file format (TIFF) files and imported into a MacIntosh IIci personal computer. These images were then printed using PowerPoint software (Microsoft Corp., Redmond, Washington) and a Tektronix Phaser II SDX dye sublimation printer (Tektronix Corp., Beaverton, Oregon).

In vitro assays. We measured EROD activity in liver slices isolated from control and βNF-treated rats in DOC as follows. Slices were preincubated for 2 hr in WEM as described above. Slices were then rinsed with EBSS, then incubated in 2 ml EBSS containing 5 µM ethoxyresorufin (ER) and 25 µM dicumarol. After the specified incubation time, the concentration of fluorescent resorufin product in the culture medium was determined by fluorescence spectrometry. We determined resorufin concentrations by comparing fluorescence intensity with a standard curve prepared from resorufin standards. All fluorescence measurements were made on a Perkin-Elmer LS-50 Luminescence Spectrofluorometer (Beaconsfield, UK) using an excitation wavelength of 530 nm and an emission wavelength of 580 nm.

Liver microsome samples were prepared by standard procedures. Microsomal protein concentrations were determined by the bicinchoninic acid method described by Smith et al. (*18*). Microsomal (alkoxyresorufin-*O*-dealkylase activity assays were performed essentially as described by Burke and Mayer (*19*) and Lubet et al. (*20*). Microsomes were allowed to preincubate for 2 min in 2 ml of 100 mM Tris-HCL (pH 7.5) containing 5 mM $MgCl_2$ and 5 µM alkoxyresorufin substrate. Reactions were initiated by adding 10 µl of 100 mM NADPH (final concentration of 500 µM NADPH) and were carried out at 37°C. Maximum EROD activities were obtained using 148 µg of control microsomal protein and 14 µg of βNF-treated microsomal protein. Maximum BROD and PROD activities were obtained using 148 µg of control microsomal protein and 140 µg of βNF-treated microsomal protein. We monitored reaction kinetics on the luminescence spectrofluorometer described above using the kinetics software package supplied with the instrument.

Slice viability. We used control rat liver slices to determine the effect of culture method (DOC versus perfusion) and the effect of treatment (EBSS control versus EBSS containing 5 µM ER and 25 µM dicumarol) on slice viability. Intracellular K^+ concentrations were measured in three slices before preincubation began (0 hr), in three slices that had been preincubated 2 hr in WEM, and in three slices from each of the culture and treatment groups at two time points (30 and 60 min). Intracellular K^+ determinations were performed as described by Fisher et al. (*21*).

Immunocytochemistry. Immunocytochemical staining of rat liver sections was performed by the method of Farin et al. (*22*) using a Vectastain ABC kit (Vector Laboratories, Burlingame, California). Briefly, acetone-fixed, 5-µm thick, paraffin sections of control and βNF-treated rat liver on poly-L-lysine coated slides were deparaffinized and rehydrated. Tissue sections were sequentially exposed to normal goat serum for 30 min to decrease nonspecific binding, previously prepared anti-CYP1A1 primary antibody for 90 min, biotinylated goat–anti-rabbit IgG secondary antibody for 60 min, avidin-conjugated horseradish peroxidase complex for 60 min, 3,3′-diaminobenzidine in Tris-saline containing H_2O_2 for 10 min, and 1% osmium tetroxide for 2 min. Between each of these components, the tissue sections were washed extensively with phosphate-buffered saline. The tissue sections were counterstained with 2% methyl green, and dehydrated, and cover slips were placed on top of the tissue sections with a drop of mounting fluid. We confirmed the specificity of the CYP1A1 antibody by Western blot analysis of control and βNF-treated HepG2 cells and rat liver (*23*). The antibody bound only to a single microsomal protein isolated from βNF-treated HepG2 cells, indicating that the antibody does not cross-react with CYP1A2 [see Farin et al. (*22*) for details of antibody preparation and specificity].

Statistical analysis. Intracellular K^+ concentrations for preincubated slices and slices that were perfused or incubated by DOC both with and without substrate at 30 and 60 min were compared by analysis of variance. EROD, PROD, and BROD activities measured by slice perfusion were

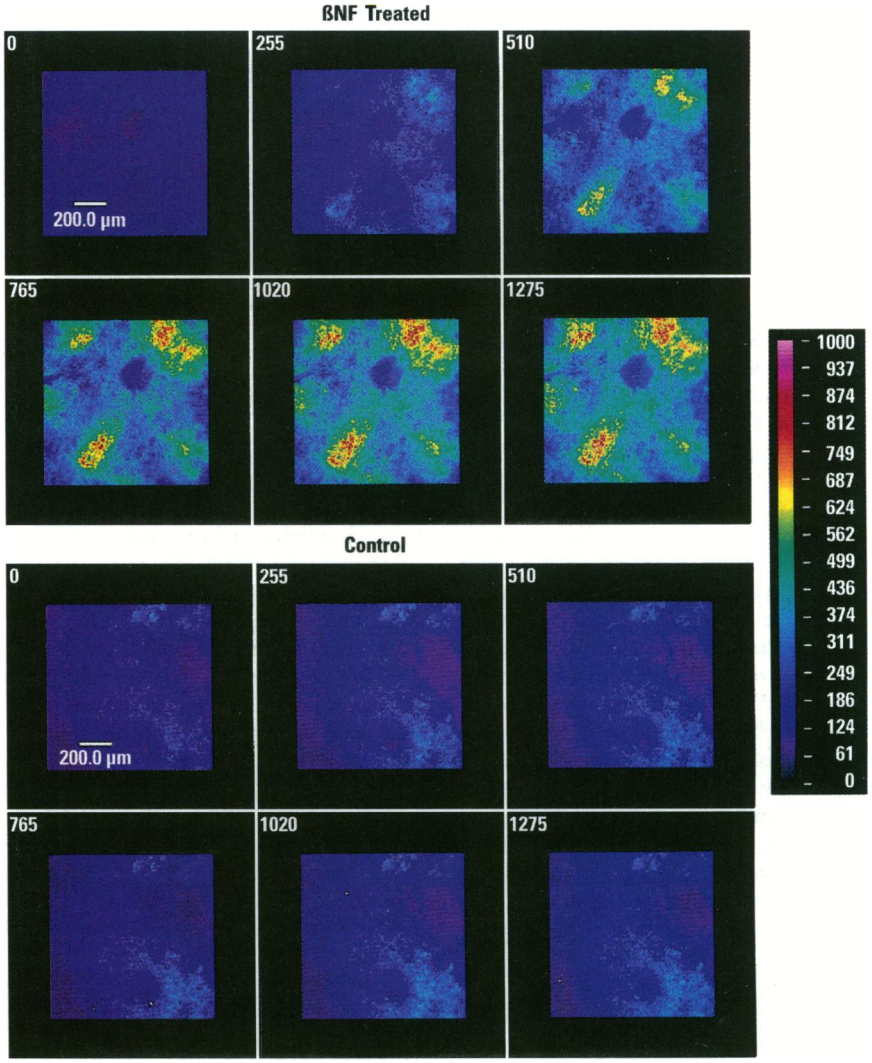

Figure 2. Comparison of ethoxyresorufin-*O*-deethylase (EROD) activity in liver slices isolated from β-naphthoflavone (βNF)-treated and control rats. Fluorescence images were acquired by confocal laser cytometry of liver slices perfused on the cytometer stage with 5 µM ethoxyresorufin (ER) as described in Materials and Methods. Numbers in the upper left-hand corner of each frame represent the time course of perfusion with ER in seconds. βNF-induced increases in CYP1A1-associated EROD activity are seen as increases from violet to red as depicted on the fluorescence intensity scale bar shown on the right.

compared by regression analysis. We used the StatView statistics program (Brain-Power Inc., Calabasas, California) for statistical analyses. Scheffe's *F*-test was used to establish significant differences.

Results

Liver slice intracellular K^+ concentrations increased from 35.4 ± 5.0 µmol K^+/g liver (mean ± SD) to 56.6 ± 5.0 µmol K^+/g liver during the 2-hr preincubation period (data not shown). Recovery of intracellular K^+ during the preincubation period is characteristic of viable liver slices (*12*). Preincubated slices that were then incubated with or without ER for 30 and 60 min by DOC at 37°C maintained 94–103% of the intracellular K^+ measured in preincubated slices. Intracellular K^+ concentrations in liver slices perfused at room temperature appeared to decrease after a 30-min perfusion (42.9 ± 7.8 and 42.4 ± 8.1 in control and ER-treated slices, respectively), then increase after a 60-min perfusion (50.0 ± 5.8 and 44.9 ± 4.1 in control and EROD-treated slices, respectively). However, when the mean intracellular K^+ values for all treatment groups (DOC versus perfusion and EBSS control versus EBSS containing 5 µM ER and 25 µM dicumarol) and preincubated slices were compared, the differences were not significant ($p = 0.05$).

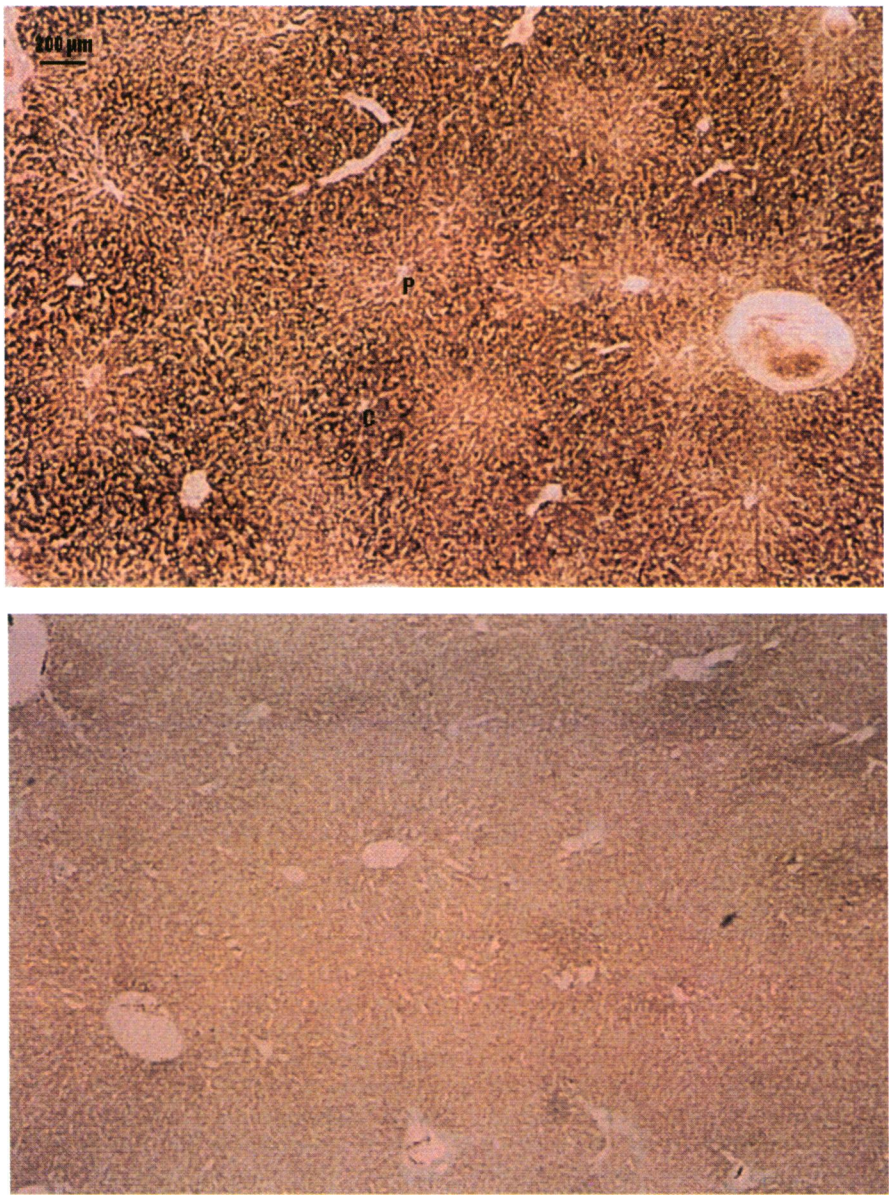

Figure 3. Comparison of CYP1A1 expression in liver sections isolated from (top) β-naphthoflavone (βNF)-treated and (bottom) control rats. Sections were subjected to immunocytochemical staining for CYP1A1 as described in Materials and Methods. βNF-induced increases in centrilobular expression of CYP1A1 are shown as dark-staining regions surrounding central veins in sections isolated from a βNF-treated rat. C, central vein; P, portal vein. ×40.

The fluorescence images in Figure 2 were collected over a period of minutes in a typical experiment in which liver slices isolated from control and βNF-treated rats were perfused on the laser cytometer stage with EBSS containing 5 µM ER. Areas of increased fluorescence are due to the formation of the fluorescent resorufin product and are indicative of high EROD activity. Whole-slice scans (data not shown) revealed a heterogeneous pattern of EROD activity, suggesting differential induction of CYP1A1 activity across regions of the liver lobule. The time elapsed during whole-slice scans made it impractical for kinetic analyses of entire slices, as fluorescence intensity increased substantially during the time required to stage-scan an entire slice (10 mm × 10 mm). Based on these kinetic considerations, we chose to scan smaller fields (1 mm × 1 mm, requiring <30 sec/scan using the fast-scanning mirror option on the ACAS). These fields contained vascular structures that appeared to be central veins. These structures were visible by light microscopy and could be targeted during initial focusing by manually positioning the slice with the computer-controlled X,Y stage. Areas of the slice where vascular structures appeared to be circular, indicating they were cut perpendicular to the slice surface, were suitable fields for resolution of the liver lobule. The size of the areas scanned by confocal laser cytometry roughly corresponds to the size of areas of distinct zonal immunocytochemical staining of CYP1A1 shown in the photomicrograph of the liver section isolated from a βNF-pretreated rat (Fig. 3).

The fluorescence images in Figure 2 show areas of intense fluorescence response in a liver slice isolated from a βNF-treated rat. The fluorescence level attained after 1275 sec of scanning in these areas is approximately 600–800 fluorescence intensity units (FIU), which is at least twofold higher than that observed in less-intense adjacent areas. Immunocytochemical data showing high levels of CYP1A1 in centrilobular areas suggest that these images depict high EROD activity in centrilobular regions of the liver slice containing what appear to be small central veins.

Perfusion of control rat liver slices with ER resulted in a low fluorescence response and reflects the relatively low EROD activity in uninduced rat liver (*9,10,16,24*). The control rat liver section in Figure 3 reveals a low, constitutive level of CYP1A1 expression that is homogenous across the different zonal regions of the liver. In contrast, the

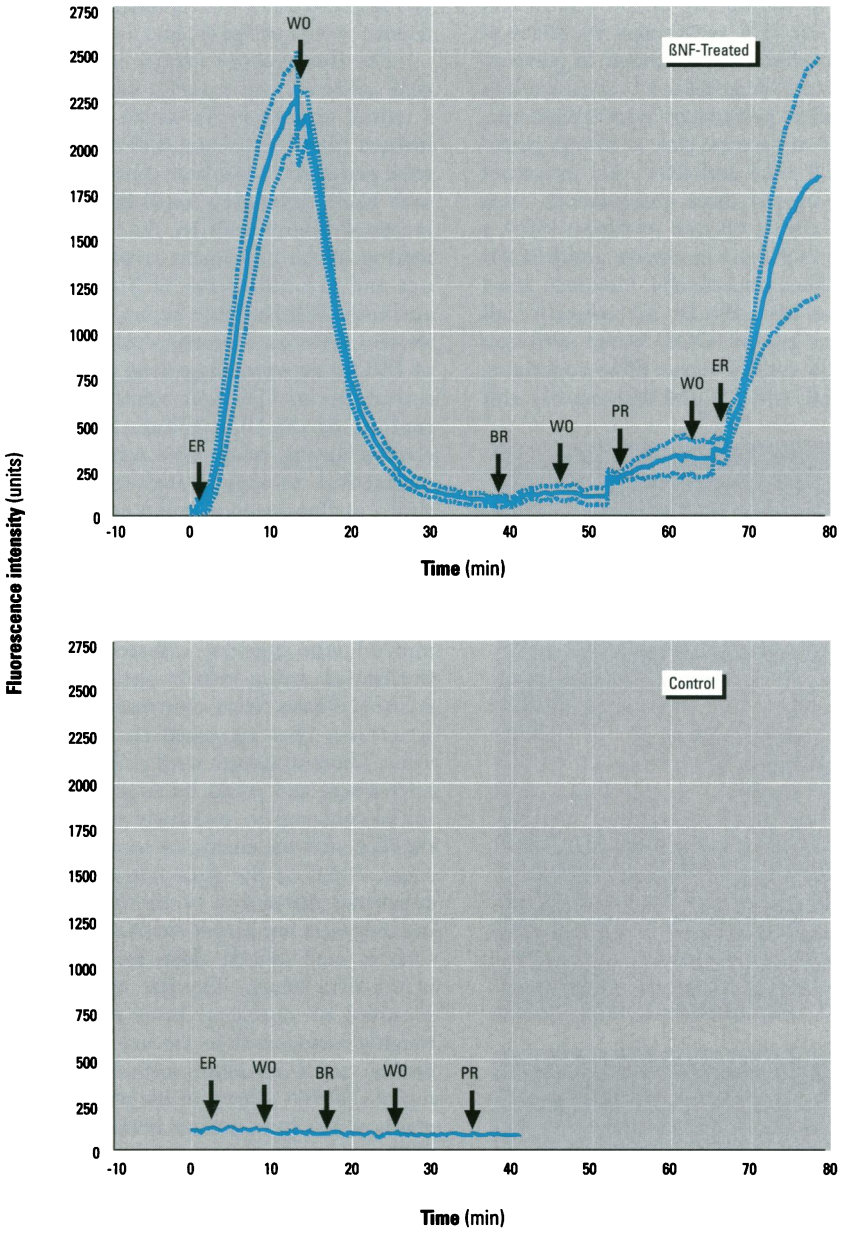

Figure 4. Sequential perfusion of liver slices isolated from β-naphthoflavone (βNF)-treated and control rats with selected alkoxyresorufin substrates (5 μM). Slices were sequentially perfused on the laser cytometer stage as described in Materials and Methods. ER , BR, and PR represent time point at which ethoxy-, benzyloxy-, or pentoxyresorufin were added to the perfusion buffer, respectively. WO (washout) represents time point at which respective substrate was removed from the perfusion buffer to wash out residual resorufin product and return fluorescence to background levels before subsequent addition of next substrate. Values represent the mean ± SD (dotted lines) of seven circular areas containing the maximum fluorescence response in βNF-treated liver slice. Control slice values were measured in one large, circular area containing maximum fluorescence response.

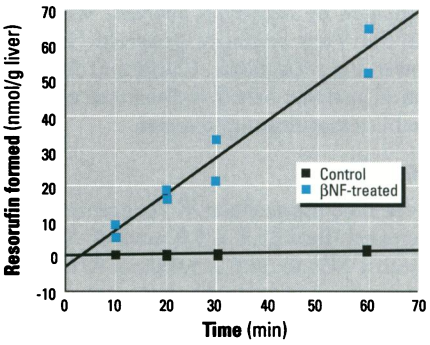

Figure 5. Comparison of ethoxyresorufin-*O*-deethylase (EROD) activity in liver slices isolated from control and β-naphthoflavone (βNF)-treated rats by dynamic organ culture. Slices were incubated with 5 μM ethoxyresorufin (ER) for 10, 20, 30, or 60 min as described in Materials and Methods. EROD activity in liver slices isolated from βNF-treated rats was linear for periods of up to 60 min, and the rate of resorufin formation was nearly 60-fold higher in treated slices than in control slices.

βNF-treated rat liver section shows a marked increase in CYP1A1 expression, but only in centrilobular regions.

To further substantiate the suggested association between high centrilobular expression of CYP1A1 and the heterogeneous fluorescence response of the βNF-treated rat liver slice perfused with ER, we sequentially perfused liver slices from control and βNF-treated rats with ER, benzyloxyresorufin (BR), and pentoxyresorufin (PR). Figure 4 demonstrates that the fluorescence response of control rat liver slices toward BR and PR is comparable to the fluorescence response observed when control slices are perfused with ER. Increases in fluorescence intensity were below the limits of quantification (10 FIU/min) for each of the three substrates in control slices. These results indicate that rat liver slices have low, constitutive levels of EROD, BROD, and PROD activity, as has been shown previously in microsomes from untreated rats (*9,24*).

In contrast to the equivalent response of control slices toward ER, BR, and PR, slices isolated from βNF-treated rats show a highly differentiated response toward these three substrates. Figure 4 shows the increase in fluorescence intensity of seven defined areas containing cells and/or groups of cells exhibiting maximum fluorescence response. The relative maximum fluorescence response of liver slices from βNF-treated rats toward ER is approximately 20-fold higher than the response toward BR and PR. The maximum rate of increase in fluorescence intensity over an approximate 3-min time period for each of the substrates in βNF-treated slices was 307, 18.5, and 16.1 FIU/min for ER, BR, and PR, respectively. These results indicate that liver slices from βNF-treated rats have high EROD activity relative to BROD and PROD activity and that EROD, BROD, and PROD activities are at least 30-, 1.8-, and 1.6-fold greater, respectively, in βNF-treated slices than in control slices.

To ensure that the lack of fluorescence response of liver slices from βNF-treated rats perfused with BR and PR was not due to possible depletion of cofactors resulting from the preceding ER perfusion, we reperfused slices with ER following BR and PR perfusion. The fluorescence response of the liver slice during the second ER perfusion approached the fluorescence response observed during the initial perfusion (Fig. 4). The maximum rate of increase in fluorescence intensity for the second ER perfu-

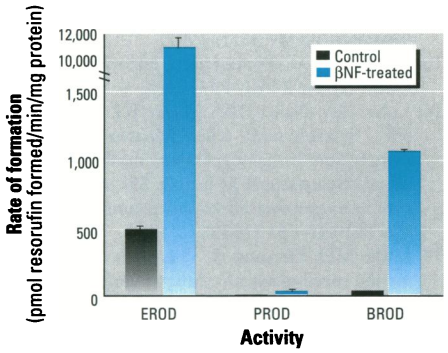

Figure 6. Comparison of alkoxyresorufin-*O*-dealkylase activities in liver microsomes isolated from control and β-naphthoflavone (βNF)-treated rats. Liver microsomes were prepared and incubated as described in Materials and Methods using a substrate concentration of 5 μM. Results are expressed as means ± SD from triplicate analyses.

sion was 193 FIU/min. Although this represents only 63% of the activity observed in the initial ER perfusion (significant at $p < 0.05$), EROD activity measured during the second ER perfusion is substantially greater than the preceding BROD and PROD activities. Taken together, these findings suggest that only a small depletion of cofactors that support *O*-dealkylase activity, such as NADPH, occurred during the 60 min preceding the second ER perfusion. The magnitude of the second ER response indicates that the low BROD and PROD activities shown in Figure 4 are more likely due to low substrate-specific isozyme expression rather than depletion of cofactors.

Figure 5 shows the regression lines for the amount of the fluorescent resorufin product formed over time by liver slices isolated from both control and βNF-treated rats incubated with 5 μM ER in DOC. The correlation coefficient for the regression line that describes the rate of resorufin formation (EROD activity) in βNF-induced liver slices indicates a high degree of linearity ($R^2 = 0.949$). This suggests, as does the second ER perfusion in Figure 4, that cofactors supporting *O*-dealkylase activity are adequately maintained in liver slices from βNF-treated rats for periods of at least 60 min. In addition, the slope of the βNF-treated regression line is nearly 60-fold greater than the slope of the control regression line.

Figure 6 further demonstrates the selective induction of EROD activity by βNF, as previously shown in whole-liver slice perfusion experiments (Fig. 4). Microsomes isolated from ββNF-treated rats had greater than 20-fold higher EROD activity than control rat liver microsomes. This is consistent with previous studies that compare microsomal EROD activity in control and βNF-treated rats (*9,24*). It is interesting to note, however, that the profile of *O*-dealkylase activities in microsomes does not parallel the activity profile seen in whole-liver slice perfusion experiments. The activity profile for liver slices isolated from βNF-treated rats could be described as EROD>>>BROD=PROD, whereas in microsomes from βNF-treated rats, the activity profile is EROD>BROD>> PROD. These differences may be due to the intact nature of the liver slice and may reflect differences in isozyme kinetics as a result of the more biologically relevant cofactor and substrate concentrations achieved in whole-cell systems.

Discussion

The fluorescence images in Figure 2 show that perfusion of liver slices isolated from βNF-treated rats with EBSS containing 5 μM ER results in an intense fluorescence response localized to specific regions of the liver lobule. Immunocytochemical staining of liver sections isolated from control and βNF-treated rats (Fig. 3) demonstrates that βNF treatment results in centrilobular induction of CYP1A1. Precision-cut liver slices incubated with ER in DOC show that slices isolated from βNF-treated rats (Fig. 5) have nearly 60-fold higher EROD activity than slices isolated from control rats. In addition, analysis of a series of alkoxyresorufin *O*-dealkylase activities in precision-cut liver slices by confocal laser cytometry (Fig. 4) shows that βNF treatment results in increased EROD activity to a much greater extent than either PROD or BROD activity. A similar response is observed in liver microsomes isolated from control and βNF-treated rats (Fig. 6), except that BROD activity was also induced to a greater extent in microsomes than in intact liver slices. Based on these findings, we conclude that the fluorescence images in Figure 2 accurately reflect high levels of centrilobular EROD activity due to region-specific induction of CYP1A1 by βNF in the rat.

βNF and 3-methylcholanthrene (MC) are prototypic inducing agents representative of a broad range of compounds such as polyaromatic hydrocarbons, coplanar polychlorinated biphenyls, and 2,3,7,8-tetrachlorodibenzo-*p*-dioxin. Treatment with these compounds results in increased expression of the *CYP1A* gene family (*2*). Baron et al. (*25*) showed by immunocytochemical techniques that treatment of male Holtzman rats with βNF (40 mg/kg) or MC (25 mg/kg) results in increased expression of CYP1A isozymes that is nearly homogeneous across the liver lobule. In addition, the relative amounts and distribution of these isozymes are the same in the right, median, left, and caudate lobes of the liver (*25*). More recently, van Sliedregt and van Bezooijen (*6*) found that the induction pattern in Brown Norway rats was dependent on dose and that at low doses of MC (2.5, 5, 7.5 and 10 mg/kg) the highest expression levels were concentrated around the central vein. Higher doses of MC (25 mg/kg) resulted in a homogeneous pattern of induction.

Based on these findings and the comparatively high dose of βNF (65 mg/kg) used in our experiments, we would expect to see a homogenous pattern of CYP1A1 induction. However, we found that sections isolated from βNF-treated Sprague-Dawley rats (Fig. 3) show very dark staining for CYP1A1 in centrilobular areas only, a pattern identical to that observed by van Sliedregt et al. (*6*) at low doses of MC.

Recent work using periportal and perivenous hepatocytes isolated by zone-restricted digitonin treatment during *in situ* perfusion have demonstrated regional differences in the constitutive expression and inducibility of a number of P450s (*4,26*). In addition, Buhler et al. (*4*) noted that the inducible forms of P450 they studied (2B1/2, 2E1, and 3A1) were generally induced in hepatocytes of the same zonal origin in which they were constitutively expressed. These findings led them to suggest that phenotypic differences exist between centrilobular and periportal hepatocytes with respect to factors that control P450 expression, causing hepatocytes of different zonal origins to respond differently to exogenous and endogenous signals.

Comparative studies investigating the phenobarbital responsiveness of rat hepatic hyperplastic nodules (HHN) have provided further evidence for phenotypic differences between centrilobular and periportal hepatocytes in factors that control P450 isozyme expression. Phenobarbital induces CYP3A1 in centrilobular hepatocytes (*23*) and CYP2B1/2 in centrilobular and midzonal hepatocytes (*23,27*). Chen et al. (*23, 28*) have demonstrated that HHNs induced by the aflatoxin B_1(AFB_1) administration protocol (*5*) arise through clonal expansion of centrilobular hepatocytes only. In contrast, HHNs induced by the Solt-Farber induction protocol (*5*) are derived from centrilobular, midzonal, and periportal hepatocytes (*28*). When HHN-bearing rats were administered phenobarbital, all AFB_1-induced HHNs expressed increased levels of CYP3A1 and CYP2B1/2 (*28*). In contrast, only a portion of Solt-Farber-induced HHNs were shown to respond to pheno-

barbital as measured by increased expression of these isozymes (*23, 28*). These findings led Chen and Eaton (*28*) to hypothesize that phenobarbital responsiveness is determined primarily by the zonal origin of precursor hepatocytes and provide indirect evidence for distinct, heritable phenotypic differences between hepatocytes of different zonal origin that control P450 expression.

At the present time, relatively little is known about factors controlling region-specific constitutive and inducible P450 isozyme activity. Anundi et al. (*26*) and Lindros et al. (*29*) have described linkages between zone-specific P450 isozyme expression and zone-specific hepatic lesions. In addition, the effects of P450 expression by HHNs on tumor promotion and progression have been well documented (*30*). These findings emphasize the importance of developing *in vitro* assays that could be used to colocalize functional P450 isozyme activity with factors governing P450 expression. Sidhu et al. (*8*) have demonstrated the ability of noninvasive scanning laser cytometry to measure CYP1A1 functional activity in hepatoma cell lines. More recently, this same group demonstrated large individual cell differences in the functional activity and the immunoreactive protein content of primary rat hepatocytes exposed to prototypic P450 inducers *in vitro* (*8,31*). The ability of scanning laser cytometry to measure functional activity in a whole-cell system led us to hypothesize that laser cytometry could be used to measure functional P450 isozyme activity in viable precision-cut liver slices and that, because the architecture of the liver lobule in liver slices remains intact, marked differences in regional activity could be observed.

In conclusion, using a well-characterized induction protocol and P450 isozyme-specific alkoxyresorufin substrates, we were able to show that confocal laser cytometry of precision-cut liver slices can be used to assess P450 isozyme-specific induction in intact liver tissue. More importantly, the method allows for the analysis of region-specific induction of P450 activities, which are difficult to determine by conventional methods. These techniques should allow for the accurate quantification of P450 enzyme activity *in situ* and, with subsequent analysis of the same slice after fixation and processing, the ability to correlate specific P450 isozyme mRNA, specific P450 isozyme protein content, or other factors, with enzyme activity on an individual cell basis. These techniques should also be amenable to examination of similar phenomena in other tissues such as lung and kidney, where heterogeneity in cellular P450 expression is also known to occur.

References

1. Guengerich FP, Shimada T. Oxidation of toxic and carcinogenic chemicals by human cytochrome P-450 enzymes. Chem Res Toxicol 4:391–407 (1991).
2. Nelson DR, Kamataki T, Waxman DJ, Guengerich FP, Estabrook RW, Feyereisen R, Gonzalez FJ, Coon MJ, Gunsalus IC, Gotoh O. The P450 superfamily: update on new sequences, gene mapping, accession numbers, early trivial names of enzymes, and nomenclature. DNA Cell Biol 12:1–51 (1993).
3. Baron J, Redick JA, Guengerich FP. An immunohistochemical study on the localization and distributions of phenobarbital- and 3-methylcholanthrene-inducible cytochromes P-450 within the livers of untreated rats. J Biol Chem 256:5931–5937 (1981).
4. Buhler R, Lindros KO, Nordling A, Johansson I, Ingelman SM. Zonation of cytochrome P450 isozyme expression and induction in rat liver. Eur J Biochem 204:407–412 (1992).
5. Chen ZY, Eaton DL. Differential regulation of cytochrome(s) P450 2B1/2 by phenobarbital in hepatic hyperplastic nodules induced by aflatoxin B1 or diethylnitrosamine plus 2-acetylaminofluorene in male F344 rats. Toxicol Appl Pharmacol 111:132–144 (1991).
6. van Sliedregt A, van Bezooijen CF. Effect of different doses of 3-methylcholanthrene on the localization of the 3-methylcholanthrene-inducible isoenzymes of cytochrome P450 within the centrilobular and periportal zones of the rat liver. Biochem Pharmacol 39:1703–1708 (1990).
7. Omiecinski CJ, Hassett C, Costa P. Developmental expression and in situ localization of the phenobarbital-inducible rat hepatic mRNAs for cytochromes CYP2B1, CYP2B2, CYP2C6, and CYP3A1. Mol Pharmacol 38:462–470 (1990).
8. Sidhu JS, Kavanagh TJ, Reilly MT, Omiecinski CJ. Direct determination of functional activity of cytochrome P-4501A1 and NADPH DT-diaphorase in hepatoma cell lines using noninvasive scanning laser cytometry. J Toxicol Environ Health 40:177–194 (1993).
9. Burke MD, Thompson S, Elcombe CR, Halpert J, Haaparanta T, Mayer RT. Ethoxy-, pentoxy- and benzyloxyphenoxazones and homologues: a series of substrates to distinguish between different induced cytochromes P-450. Biochem Pharmacol 34:3337–3345 (1985).
10. Nakajima T, Elovaara E, Park SS, Gelboin HV, Hietanen E, Vainio H. Monoclonal antibody-directed characterization of benzene, ethoxyresorufin and pentoxyresorufin metabolism in rat liver microsomes. Biochem Pharmacol 40:1255–1261 (1990).
11. Krumdieck CL, dos Santos JE, Ho KJ. A new instrument for the rapid preparation of tissue slices. Anal Biochem 104:118–123 (1980).
12. Smith PF, Gandolfi AJ, Krumdieck CL, Putnam CW, Zukoski CF, Davis WM, Brendel K. Dynamic organ culture of precision liver slices for in vitro toxicology. Life Sci 36:1367–1375 (1985).
13. Gahwiler BH. Organotypic monolayer cultures of nervous tissue. J Neurosci Methods 4:329–342 (1981).
14. Forscher P, Kaczmarek LK, Buchanan JA, Smith SJ. Cyclic AMP induces changes in distribution and transport of organelles within growth cones of Aplysia bag cell neurons. J Neurosci 7:3600–3611 (1987).
15. Ernster L. DT-diaphorase: a historical review. Chem Scripta 27A:1–13 (1987).
16. Lubet RA, Nims RW, Mayer RT, Cameron JW, Schechtman LM. Measurement of cytochrome P-450 dependent dealkylation of alkoxyphenoxazones in hepatic S9s and hepatocyte homogenates: effects of dicumarol. Mutat Res 142:127–131 (1985).
17. Burke MD, Orrenius S. The effect of albumin on the metabolism of ethoxyresorufin through O-deethylation and sulfate conjugation using isolated rat hepatocytes. Biochem Pharmacol 27:1533–1538 (1978).
18. Smith PK, Krohn RI, Hermanson GT, Mallia AK, Gartner FH, Provenzano MD, Fujimoto EK, Goeke NM, Olson BJ, Klenk DC. Measurement of protein using bicinchoninic acid. Anal Biochem 150:76–85 (1985).
19. Burke MD, Mayer RT. Ethoxyresorufin: direct fluorimetric assay of a microsomal O-dealkylation which is preferentially inducible by 3-methylcholanthrene. Drug Metab Dispos 2:583–588 (1974).
20. Lubet RA, Mayer RT, Cameron JW, Nims RW, Burke MD, Wolff T, Guengerich FP. Dealkylation of pentoxyresorufin: a rapid and sensitive assay for measuring induction of cytochrome(s) P-450 by phenobarbital and other xenobiotics in the rat. Arch Biochem Biopys 238:43–48 (1985).
21. Fisher R, Smith PF, Sipes IG, Gandolphi AJ, Krumdieck CL, Brendel K. Toxicity of chlorobenzenes in cultured rat liver slices. In Vitro Toxicol 3:181–194 (1990).
22. Farin FM, Omiecinski CJ. Regiospecific expression of cytochrome P-450s and microsomal epoxide hydrolase in human brain tissue. J Toxicol Environ Health 40:317–335 (1993).
23. Chen ZY, Farin F, Omiecinski CJ, Eaton DL. Association between growth stimulation by phenobarbital and expression of cytochromes P450 1A1, 1A2, 2B1/2 and 3A1 in hepatic hyperplastic nodules in male F344 rats. Carcinogenesis 13:675–682 (1992).
24. Lubet RA, Syi JL, Nelson JO, Nims RW. Induction of hepatic cytochrome P-450 mediated alkoxyresorufin O-dealkylase activities in different species by prototype P-450 inducers. Chem Biol Interact 75:325–339 (1990).
25. Baron J, Redick JA, Guengerich FP. Effects of 3-methylcholanthrene, beta-naphthoflavone, and phenobarbital on the 3-methylcholanthrene-inducible isozyme of cytochrome P-450 within centrilobular, midzonal, and periportal hepatocytes. J Biol Chem 257:953–957 (1982).
26. Anundi I, Lahteenmaki T, Rundgren M, Moldeus P, Lindros KO. Zonation of acetaminophen metabolism and cytochrome P450 2E1-mediated toxicity studied in isolated periportal and perivenous hepatocytes. Biochem Pharmacol 45:1251–1259 (1993).
27. Bars RG, Bell DR, Elcombe CR, Oinonen T, Jalava T, Lindros KO. Zone-specific inducibility of cytochrome P450 2B1/2 is retained in isolated perivenous hepatocytes. Biochem J 282:635–638 (1992).
28. Chen ZY, Eaton DL. Association between responsiveness to phenobarbital induction of CYP2B1/2 and 3A1 in rat hepatic hyperplastic nodules and their zonal origin. Environ Health Perspect 101(suppl 5):185–190 (1993).
29. Lindros KO, Cai YA, Penttila KE. Role of

ethanol-inducible cytochrome P450 IIE1 in carbon tetrachloride-induced damage to centrilobular hepatocytes from ethanol-treated rats. Hepatology 12:1092–1097 (1990).
30. Chen ZY, White CC, Eaton DL. Decreased expression of cytochrome P450 mRNAs and related steroid hydroxylation activities in hepatic hyperplastic nodules in male F344 rats. Toxicol Appl Pharmacol 123:151–159 (1993).
31. Sidhu JS, Kavanagh TJ, Farin FM, Omiecinski CJ. Use of scanning laser cytometry to determine functional activity and immunoreactive protein associated with phenobarbital- and beta-napthoflavone-inducible CYP genes in primary rat hepatocytes. In Vitro Toxicol 7:225–242 (1994).